2-2005

Anisotropic Interfacial Free Energies of the Hard-Sphere Crystal–Melt Interfaces

Yan Mu
Iowa State University

Andrew Houk
Iowa State University

Xueyu Song
Iowa State University, xsong@iastate.edu

Anisotropic Interfacial Free Energies of the Hard-Sphere Crystal–Melt Interfaces

Abstract

We present a reliable method to define the interfacial particles for determining the crystal–melt interface position, which is the key step for the crystal–melt interfacial free energy calculations using capillary wave approach. Using this method, we have calculated the free energies γ of the fcc crystal-melt interfaces for the hard-sphere system as a function of crystal orientations by examining the height fluctuations of the interface using Monte Carlo simulations. We find that the average interfacial free energy $\gamma_0 = 0.62 \pm 0.02 k_BT/\sigma^2$ and the anisotropy of the interfacial free energies are weak, $\gamma_{100} = 0.64 \pm 0.02$, $\gamma_{110} = 0.62 \pm 0.02$, $\gamma_{111} = 0.61 \pm 0.02 k_BT/\sigma^2$. The results are in good agreement with previous simulation results based on the calculations of the reversible work required to create the interfaces (Davidchack and Laird, *Phys. Rev. Lett.* **2000**, *85*, 4571). In addition, our results indicate $\gamma_{100} > \gamma_{110} > \gamma_{111}$ for the hard-sphere system, similar to the results of the Lennard–Jones system.

Disciplines
Chemistry

Anisotropic Interfacial Free Energies of the Hard-Sphere Crystal−Melt Interfaces[†]

Yan Mu, Andrew Houk, and Xueyu Song*

Department of Chemistry, Iowa State University, Ames, Iowa 50011

Received: August 17, 2004; In Final Form: December 28, 2004

We present a reliable method to define the interfacial particles for determining the crystal−melt interface position, which is the key step for the crystal−melt interfacial free energy calculations using capillary wave approach. Using this method, we have calculated the free energies γ of the fcc crystal-melt interfaces for the hard-sphere system as a function of crystal orientations by examining the height fluctuations of the interface using Monte Carlo simulations. We find that the average interfacial free energy $\gamma_0 = 0.62 \pm 0.02 k_B T/\sigma^2$ and the anisotropy of the interfacial free energies are weak, $\gamma_{100} = 0.64 \pm 0.02$, $\gamma_{110} = 0.62 \pm 0.02$, $\gamma_{111} = 0.61 \pm 0.02 k_B T/\sigma^2$. The results are in good agreement with previous simulation results based on the calculations of the reversible work required to create the interfaces (Davidchack and Laird, *Phys. Rev. Lett.* **2000,** *85,* 4571). In addition, our results indicate $\gamma_{100} > \gamma_{110} > \gamma_{111}$ for the hard-sphere system, similar to the results of the Lennard−Jones system.

I. Introduction

The interface between a crystal and its melt is one of the most important subjects with considerable studies in physics, chemistry, and material sciences. In particular, there has been a persistent interest focusing on the calculation of the interfacial free energy γ, due to both its fundamental physics value and the practical applications for determining material properties. As a matter of fact, although many theoretical and experimental studies had been done, fundamental understanding and detailed microstructural description of the interface between a crystal and its melt are still in its early stage.[1,2]

Theoretically, the primary approach to study the structure and thermodynamics of the crystal−melt interface has been density-functional theory (DFT).[3−6] However, for the hard-sphere system considered in this paper, the value of the interfacial free energy γ obtained depends very much on the approximations used and the density profile parametrizations employed in the DFT studies, ranging from $0.25 k_B T/\sigma^2$ to $4.00 k_B T/\sigma^2$.[7] The DFT studies also disagree dramatically in the degree of orientation dependence of the interfacial free energies.

Experimentally, the interfacial free energy γ can be estimated from measurements of crystal nucleation rates interpreted through classical nucleation theory. After the studies of γ for a number of materials, Turnbull[8] found a strong empirical correlation between the interfacial free energy and the latent heat of fusion per unit area given by the relation $\gamma \approx C_T \Delta_f H \rho_s^{2/3}$, where ρ_s is the number density of the solid phase and C_T is the Turnbull coefficient taking 0.45 for most metals and 0.32 for other mostly nonmetallic materials. An interesting physical argument has been proposed by Laird to explain the Turnbull rule.[9] Recently, some experiments[10,11] of the crystallization kinetics of colloidal systems that closely approximate the hard-sphere system have been interpreted within classical nucleation theory to provide an experimental estimate for the interfacial free energy of the hard-sphere system of $\gamma \approx (0.55$

$\pm~0.02) k_B T/\sigma^2$.[12] This result is in good agreement with that predicted using Turnbull's empirical relationship above.[7] However, the method of measuring crystal nucleation rates cannot be used to determine the anisotropy of the interfacial free energy, and the values obtained are not very accurate due to the approximations inherent in classical nucleation theory. More accurate and direct techniques have been developed, examining the shape of the interface where it intersects with a grain boundary. Unfortunately, such experiments are difficult, and so far only a few materials have been studied. For example, experimentally determined γ of bismuth, 61.3×10^{-3} J/m^2, is relatively independent of crystal orientation and for Al the anisotropy is about 2%,[13,14] but a direct comparison with hard-sphere system results is not straightforward because of the long-range attraction interactions.

The determination of the interfacial free energy γ may also be obtained using computer simulations. In recent years, the calculations of crystal−melt interfacial free energies have been performed for Lennard−Jones and hard-sphere systems by using a number of techniques of computer simulations. For the Lennard−Jones system, Broughton and Gilmer[15] used a cleaving potential approach. In that work, a series of fictitious external cleaving potential are used to create interfaces in bulk solid and liquid phases and then to bring the interfaces into contact in a nearly reversible manner. The virtual work required to create the crystal−melt interface is then directly related to the interfacial free energy. However, this early work was unable to accurately determine the anisotropy of the interfacial free energies. Recently, Davidchack and Laird applied a variation of this technique to calculate the interfacial free energy of the hard-sphere and Lennard−Jones systems using molecular dynamic (MD) simulations and provided sufficient accuracies of anisotropy of the interfacial free energies.[16,17]

An alternate approach via simulations, capillary wave method,[2,18−20] has been used and applied to a number of model systems of metals in the past few years.[21−26] The approach is based on the fact that most crystal−melt interfaces of interest are flat and homogeneous over macroscopic length scales but

Free Energies of Hard-Sphere Crystal−Melt Interfaces

J. Phys. Chem. B, Vol. 109, No. 14, 2005 **6501**

are rough and inhomogeneous over microscopic length scales. Therefore, the magnitude of the height fluctuations of the interface depends on the stiffness of the interfaces which is related to the interfacial free energy. With this method, Morris and Song[26] calculated the interfacial free energies for the Lennard−Jones system using molecular dynamic simulations, and the results are in good agreement with calculations of the interfacial free energies based upon the cleaving potential approach.[17] But the order of orientation-dependent interfacial free energies is different from the result of a hard-sphere system.[16] In this work, we used this approach to calculate the interfacial free energies for a hard-sphere system via Monte Carlo simulations. It is found that the orientation-dependent interfacial free energies have the same order as those in the Lennard−Jones system, but overall the agreement between these two methods is good. Furthermore, we have developed a reliable way to determine the interface position which is the key step for the capillary wave method.

The paper is organized as the following. In section II, we briefly outline the capillary wave approach and the rationale of our determination of the interface position. In section III, simulation results are presented with discussions related to previous works. Some conclusions are drawn in section IV based upon our results.

II. Capillary Wave Approach

Consider a two-dimensional crystal−melt interface which is divided by grids with grid sizes Δ_y and Δ_z; the deviation of the interface from its average position can be defined by a height function $h(\mathbf{r}_{ij})$, where $\mathbf{r}_{ij} = i\Delta_y\hat{y} + j\Delta_z\hat{z}$ denotes the position on the interface. As is well-known, it is the essential idea of capillary wave theory that the free energy cost of interfacial height fluctuations is proportional to the increase in the interfacial area caused by the fluctuations.[2] Assuming that the gradients $\partial h/\partial y$ and $\partial h/\partial z$ are very small, this can be written as

$$\Delta F_{CW} = \frac{\tilde{\gamma}(\theta)}{2}\int\int\left[\left(\frac{\partial h}{\partial y}\right)^2 + \left(\frac{\partial h}{\partial z}\right)^2\right]\mathrm{d}y\mathrm{d}z \qquad (1)$$

where $\tilde{\gamma}(\theta)$ is the interfacial stiffness governing fluctuations in the height of the crystal−melt interface and θ gives the orientation of the interface. The Fourier transform of interfacial height function $h(\mathbf{r}_{ij})$ may be defined by

$$h_{\mathbf{q}} = \frac{\Delta_y\Delta_z}{\sqrt{A}}\sum_{ij}h_{ij}\exp(iq\cdot\mathbf{r}_{ij}) \qquad (2)$$

where A is the area of the interface. In most of simulations using the capillary wave method, the y-direction is very narrow so that the z-direction is long enough to probe the long wavelength fluctuations, which is essential to extract out the stiffness within a reasonable computational time. Thus, the simulation system is a quasi-one-dimensional system. With this in mind, the interfacial free energy in the Fourier space then becomes

$$\Delta F_{CW} = \frac{\tilde{\gamma}(\theta)}{2}\sum_q q^2|h_q|^2 \qquad (3)$$

From the equipartition theorem, one can obtain[2]

$$\langle|h_q|^2\rangle^{-1} = \frac{\tilde{\gamma}(\theta)q^2}{k_B T} \qquad (4)$$

The interfacial stiffness $\tilde{\gamma}(\theta)$ is related to the interfacial free

TABLE 1: Summary of the Interfaces Simulated, Including the Short Direction (the *y* Direction in the Text) in the Simulations[a]

interface	short direction	interfacial free energy	interfacial stiffness
(100)	[001]	$\gamma_0(1 + {}^2/_5\epsilon_1 + {}^4/_7\epsilon_2)$	$\gamma_0(1 - {}^{18}/_5\epsilon_1 - {}^{80}/_7\epsilon_2)$
(110)	[001]	$\gamma_0(1 - {}^1/_{10}\epsilon_1 - {}^{13}/_{14}\epsilon_2)$	$\gamma_0(1 + {}^{39}/_{10}\epsilon_1 + {}^{155}/_{14}\epsilon_2)$
(110)	[$\bar{1}$10]	$\gamma_0(1 - {}^1/_{10}\epsilon_1 - {}^{13}/_{14}\epsilon_2)$	$\gamma_0(1 - {}^{21}/_{10}\epsilon_1 + {}^{365}/_{14}\epsilon_2)$
(111)	[$\bar{1}$10]	$\gamma_0(1 - {}^4/_{15}\epsilon_1 + {}^{64}/_{63}\epsilon_2)$	$\gamma_0(1 + {}^{12}/_5\epsilon_1 - {}^{1280}/_{63}\epsilon_2)$

[a] In this paper, we choose that the x direction is normal to the interface, the y and z directions are the short and long directions in the interface, respectively. The equations for interfacial stiffness in terms of γ_0 and the anisotropy parameters defined by eq 6 are shown.

energy $\gamma(\theta)$ by

$$\tilde{\gamma}(\theta) = \gamma(\theta) + \gamma''(\theta) \qquad (5)$$

For an isotropic system, the interfacial stiffness reduces back to the interfacial free energy. For an anisotropic system, in terms of the normal vector $\mathbf{n} = (n_1, n_2, n_3)$ to the crystal−melt interface, the interfacial free energy may be written as[26]

$$\gamma(\mathbf{n}) = \gamma_0\left[1 + \epsilon_1\left(\sum_i n_i^4 - \frac{3}{5}\right) + \right.$$
$$\left. \epsilon_2\left(3\sum_i n_i^4 + 66n_1^2 n_2^2 n_3^2 - \frac{17}{7}\right)\right] \qquad (6)$$

From this equation, we can derive equations relating the interfacial stiffnesses and free energies; the derived equations are given in Table 1. From Table 1, it can be clearly seen that the prefactors of the anisotropy parameters ϵ_1 and ϵ_2 are much larger for the stiffness than the free energy; that is, the interfacial stiffness is more anisotropic.[21−26] Through examining the more anisotropic interfacial stiffness, we can determine the values of the anisotropy parameters ϵ_1 and ϵ_2 more accurately. Thus, this is a sensitive method to determine the anisotropy of the interfacial free energies.

The key step of the capillary wave method is how to calculate the height function of the crystal−melt interfaces. In this paper, we developed a reliable method to define the interfacial particle to determine the position of the crystal−melt interface.

To get a height function derived from atomic configurations, we first define a local order parameter for each particle. Following the method in ref 25, we choose a set of N_q wave vectors $\vec{q}_i$ satisfying $\exp(i\vec{q}\cdot\vec{r}) = 1$ for any vector $\vec{r}$ connecting the nearest neighbors in a perfect fcc lattice. We omit one of each pair of antiparallel wave vectors and thus $N_q = 6$. Then we define the local order parameter as

$$\phi = \left|\frac{1}{N_q}\frac{1}{Z_{nn}}\sum_{\vec{r}}\sum_{\vec{q}}\exp(i\vec{q}\cdot\vec{r})\right|^2 \qquad (7)$$

where the sum on $\vec{r}$ runs over each of Z_{nn} nearest neighbors between the first- and second-neighbor shells in a perfect lattice. This order parameter will be one for a perfect fcc lattice and less than one otherwise. To reduce the effects of molecular vibrations due to thermal fluctuations and to improve the discrimination between the liquid and solid phases, an averaged local order parameter $\bar{\phi}$ is defined for each particle:[25]

$$\bar{\phi}_i = \frac{1}{Z_{nn} + 1}(\phi_i + \sum_j\phi_j) \qquad (8)$$

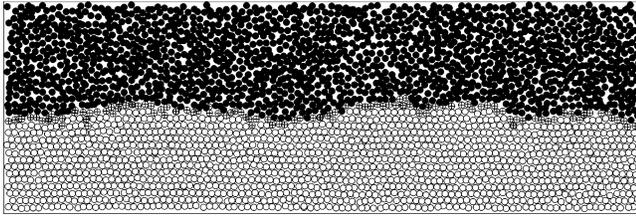where j runs over all Z_{nn} nearest neighbors of particle i. This

Figure 1. A snapshot of the system with one (111) interface generated from Monte Carlo simulations detailed in section III. The solid circles represent the liquid particles, while the open circles correspond to the solid particles. The interfacial particles are indicated by open circles with cross.
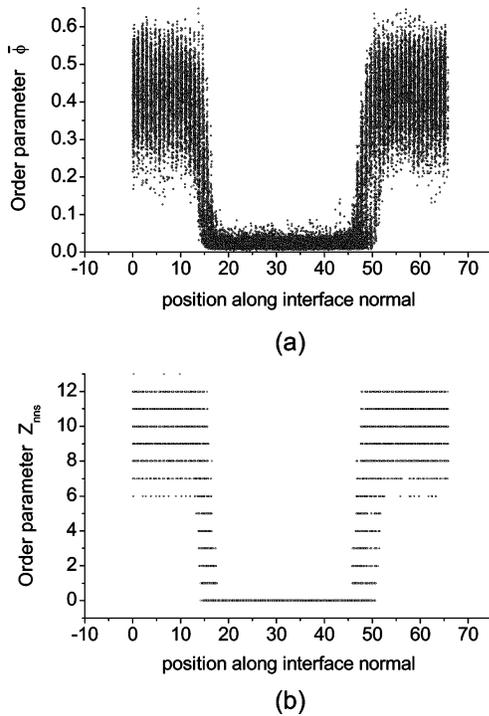

Figure 2. (a) Order parameter $\bar{\phi}$ vs position for each particle in an instantaneous configuration of two (111) interfaces (shown in Figure 1). The center region, where the order parameter is small, is the liquid region, while the regions where $\bar{\phi}$ is large correspond to the crystal region. (b) Order parameter Z_{nns} vs position for each particle in the same configuration. The particles with the order parameter $Z_{nns} = 0$ correspond to the liquid particles, while the particles with $Z_{nns} \geq Z_s$ (= 7) correspond to the solid particles. The particles that have the values of the order parameter $0 < Z_{nns} < Z_s$ correspond to the interfacial particles.

procedure helps to eliminate the difference of the local order parameters between the particle and its environment due to thermal fluctuations.

Figure 1 shows a snapshot of the system with one (111) interface, and Figure 2a shows the corresponding local order parameter $\bar{\phi}_i$ of each particle in the snapshot. From Figure 2a, it can be seen that the value of the local order parameter of the liquid phase is small, while the solid phase has the local order parameter with large values. However, only with the order parameter $\bar{\phi}_i$, it is difficult to identify the interfacial particles reliably. As the determination of interfacial particles leads to the interface position and the stiffness is sensitive to the position of the interface (cf Figure 4), a reliable way to determine these interfacial particles is crucial for the accurate extraction of the stiffness.

To define the interfacial particles, we first take a certain value $\bar{\phi}_s$ as a threshold value of the order parameter for the solid phase; that is, the particles with the order parameter $\bar{\phi} \geq \bar{\phi}_s$ belong to

TABLE 2: System Geometries and Number of Particles in Simulations and Resultant Interfacial Stiffnesses $\bar{\gamma}$ along with the Fitted Interfacial Stiffnesses from the Anisotropy Parameters ϵ_1 and ϵ_2[a]

interface	geometry	number of particles	interfacial stiffness from simulation	fitted interfacial stiffness with ϵ_1, ϵ_2
(100)[001]	$66.28 \times 6.26 \times 109.58$	44 800	0.55	0.55
(110)[001]	$70.20 \times 6.26 \times 88.58$	38 400	0.71	0.71
(110)[$\bar{1}$10]	$70.21 \times 6.64 \times 93.96$	43 200	0.49	0.43
(111)[$\bar{1}$10]	$65.81 \times 6.64 \times 95.87$	41 400	0.80	0.80

[a] The geometries are shown with all lengths in units of σ, while all interfacial stiffnesses are in units of k_BT/σ^2.

the solid phase. According to this basic criterion, we can calculate the number Z_{nns} of the nearest neighboring solid particles for each particle. Figure 2b shows the number Z_{nns} of the nearest neighboring solid particles of each particle in the same configuration as that in Figure 2a. And now we can define the other threshold value Z_s as a new criterion to identify the solid particles; that is, the particles with $Z_{nns} \geq Z_s$ are solid particles. In this paper, we choose $Z_s = 7$. For a perfect fcc crystal, each particle has 12 nearest neighbors. Considering the effects of instantaneous molecular vibrations due to thermal fluctuations, the particles which are surrounded by more than half of the 12 nearest neighbors are taken as solid particles. Thus, we choose $Z_s = 7$ here. In fact, the results are quite robust with respect to other reasonable choices of Z_s. For example, with the choice of $\bar{\phi}_s = 0.15$ for the (111) interface, as in Figure 4 the stiffness changes are within 4% if Z_s varies from 4 to 7.

With these two criteria, we can define the particles with the local order parameter $\bar{\phi}_i < \bar{\phi}_s$ and at the same time the number of the nearest neighboring solid particles $0 < Z_{nns} < Z_s$ as the interfacial particles. That is, the particles that have a small local order parameter and at the same time are next to solid particles are defined as interfacial particles. Thus, the intrinsic interface between the solid and liquid phases can be determined reliably by those interfacial particles. It can be easily understood that the value of Z_{nns} for each particle depends on the criterion $\bar{\phi}_s$. Thus, the critical parameter $\bar{\phi}_s$ is the only basic and crucial parameter in this method. A reliable method to determine this crucial parameter $\bar{\phi}_s$ is presented in section III. With this method, we evaluate the height function $h(x)$ of the crystal−melt interfaces and calculate the anisotropic interfacial free energies for the hard-sphere system. Our results clearly indicate that the anisotropy is weak but can be accurately resolved using this approach due to the sensitivity of the height fluctuations of the interface on the anisotropy.

III. Simulation Results and Discussion

In this paper, we studied the fcc crystal−melt interfaces of the hard-sphere system using Monte Carlo simulations with NPT ensemble. First, pure crystal and liquid phases are simulated separately with periodic boundary conditions, which have the density appropriate for the bulk phase at the melting pressure $P = 11.57$.[27] Subsequently, the crystal and liquid systems are joined together to create two crystal−melt interfaces. Four different crystal−melt interface simulations are performed; these geometries are summarized in Table 2. The simulation boxes are chosen to be narrow in the [001] direction ($4a_0$) or the [$\bar{1}$10] direction ($3\sqrt{2}a_0$). The choice of this quasi-one-dimensional geometry ensures that the height fluctuations of the interface are essentially functions of only one direction, which makes the analysis easier. In this paper, we choose that the x direction
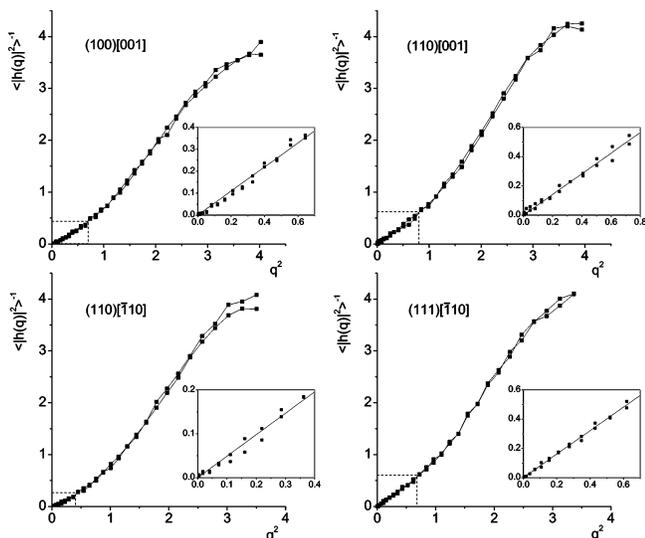
Free Energies of Hard-Sphere Crystal−Melt Interfaces

J. Phys. Chem. B, Vol. 109, No. 14, 2005 **6503**

Figure 3. Inverse of the average squared amplitude of the height fluctuations, $\langle|hq|^2\rangle^{-1}$ vs q^2, for different crystal−melt interface orientations. Each orientation includes two interfaces. The values of $\langle|hq|^2\rangle^{-1}$ are calculated for the case of $\bar{\phi}_s = 0.15$ as a result of a procedure shown in Figure 4. In the insets, the solid lines are the fit to small q portions (long wavelength modes), and the linear behavior indicates the validity of the capillary wave method. The error bars are of the order of the size of the symbols.

Figure 4. Dependence of the interfacial stiffness on the crucial parameter $\bar{\phi}_s$ for different crystal−melt interface orientations.

is normal to the interface and the y and z directions are the short and long directions in the interface, respectively. The system is run for 200 000 MC steps at the melting pressure to be equilibrated and run for 500 000 MC steps for data collection. The configurations of the system are stored every 100 MC steps during the run for data collection.

Using the above method of defining the interfacial particles, we can determine the discrete height function of the crystal−melt interface by simply calculating the average position of all the interfacial particles in each grid. To obtain good spatial resolution and at the same time to ensure that there are sufficient interfacial particles in each grid to define the height function, we choose Δ_y, $\Delta_z \approx a_0$ (a_0 is the lattice constant of fcc crystal). The values of $\langle|h_q|^2\rangle^{-1}$ are calculated for each of the geometries for the case of $\bar{\phi}_s = 0.15$, and the results are shown in Figure 3. As can be seen in Figure 3, although the global curves are not straight lines as anticipated in eq 4, in the small q region (the long wavelength modes) the simulation results follow the linear behavior, which indicates the roughness of the interfaces with Gaussian statistics. In fact, because the simulation system is a quasi-one-dimensional geometry structure ($L_z \gg L_y$), the height fluctuations in the short direction (y direction) are neglected, which suggests that the height fluctuations within the equal length region in the long direction (z direction) should also be neglected; that is, only the small q modes of $q < 2\pi/L_y$ are valid ($2\pi/L_y \approx 1$ in our case). The deviation for large q depends on the details of the method of calculating the height function of the interface and the inherent nonlinear behavior of particle's motion at short length scale. In addition, for the very long wavelength modes which can be comparable with the length of the long direction of simulation system, the deviation is due to the fact that these modes need very long relaxation and sampling time to be converged. Thus, by fitting the small q (long wavelength) portion with best linearity to the form given in eq 4 for each of the different interface orientations, we obtained the interfacial stiffness from the slope of the fitted straight line. However, the values for the stiffnesses found from the fittings depend on the choice of the parameters to define
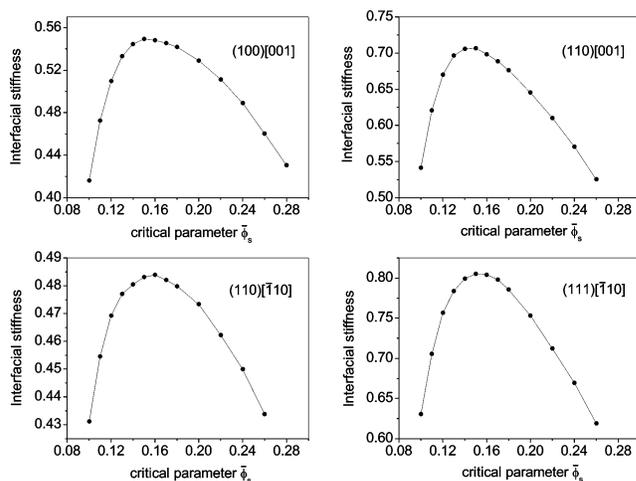
the interface position. We have found the crucial parameter is $\bar{\phi}_s$ in our case, and a reliable procedure for the choice of $\bar{\phi}_s$ is given below.

As discussed above, the critical parameter $\bar{\phi}_s$ is the only basic and crucial parameter to define the interfacial particles, in turn, the interface position. However, the choice of the value of $\bar{\phi}_s$ is not reliable if it is chosen directly from Figure 2a by visual inspection as done previously. On one hand, if the value of the critical parameter $\bar{\phi}_s$ is chosen to be too small, it will occur inevitably that a number of particles which essentially belong to liquid phase at equilibrium are taken as the interfacial particles; on the other hand, if the value of $\bar{\phi}_s$ is too large, the particles essentially belonging to solid phase are regarded as the interfacial particles. In both cases, the profile of the interface is changed dramatically by those pseudo interfacial particles, and accordingly, the height fluctuations of the interface become stronger due to greater noise, which results in the fact that the calculated results of the interfacial stiffnesses are smaller than the true value. Thus, there should exist an intermediate value for the critical parameter $\bar{\phi}_s$ by which the position of the interface can be determined relatively more accurately, and the corresponding calculated results of the interfacial stiffnesses should have a maximum. To determine the value of the parameter $\bar{\phi}_s$, we calculated the interfacial stiffnesses for different interface orientations with different $\bar{\phi}_s$. The dependences of the interfacial stiffness on the crucial parameter $\bar{\phi}_s$ for different interfaces are shown in Figure 4. From Figure 4, it can be clearly seen that the interfacial stiffnesses of all interfaces depend very much on the critical parameter $\bar{\phi}_s$ and have distinct peaks around $\bar{\phi}_s = 0.15$, all indicating that the appropriate value of this critical parameter is $\bar{\phi}_s = 0.15$. Therefore, the corresponding peak values are the best estimate of the equilibrium interfacial stiffnesses. Results based on the choice of $\bar{\phi}_s = 0.15$ are listed in Table 2.

All interfacial stiffnesses from simulations should be used with equations given in Table 1 to calculate the values of the parameters γ_0, ϵ_1, and ϵ_2 by least-squares fitting. But, here, we calculated the parameters using the three stiffnesses of (100)[001], (110)[001], and (111)[$\bar{1}$10] interfaces due to the fact that their $\langle|h_q|^2\rangle^{-1}$ curves have better linearity in the small q region. This procedure yields $\gamma_0 = 0.62$, $\epsilon_1 = 0.056$, and $\epsilon_2 = -0.0073$. The fitted interfacial stiffnesses of different crystal−melt interfaces with these parameters are given in Table 2. We also calculated the interfacial free energies of different interfaces with various orientations using these parameters according to the equations given in Table 1. These results can be compared

6504 *J. Phys. Chem. B, Vol. 109, No. 14, 2005*

Mu et al.

TABLE 3: Comparison with the Results of Davidchack and Larid for Interfacial Free Energies of Different Crystal−Melt Interface Orientations (All Interfacial Free Energies Are in Units of k_BT/σ^2)

	current work	Davidchack and Larid
γ_0	0.62 ± 0.02	0.61 ± 0.01
γ_{100}	0.64 ± 0.02	0.62 ± 0.01
γ_{110}	0.62 ± 0.02	0.64 ± 0.01
γ_{111}	0.61 ± 0.02	0.58 ± 0.01

with the results of Davidchack and Larid[16] based on the cleaving potential method, which is shown in Table 3.

As can be seen in Table 3, the average interfacial free energy $\gamma_0 = 0.62 k_BT/\sigma^2$ of the current work is in very good agreement with $0.61 k_BT/\sigma^2$ from Davidchack and Larid using the cleaving potential method via simulation and $0.616 k_BT/\sigma^2$ from the classical nucleation theory estimate.[28] However, there are some differences in the interfacial free energies of different interface orientations between our results and that of Davidchack and Larid. Both calculations show that the interfacial free energies are slightly anisotropic and the (111) interface has the lowest interfacial free energy, but for the (100) and (110) interfaces, our results indicate $\gamma_{100} > \gamma_{110}$, in contrast to $\gamma_{100} < \gamma_{110}$ of the result from Davidchack and Larid. Our results indicate that for the hard-sphere system the order of the interfacial free energies of different crystal−melt interface orientations is $\gamma_{100} > \gamma_{110} > \gamma_{111}$, which is similar to the results of the Lennard−Jones system.[17,26,29]

IV. Conclusion

In summary, we developed a reliable method to define the interfacial particles to determine the position of the intrinsic crystal−melt interface and have computed the height fluctuations of the interface from different crystal−melt orientations using the Monte Carlo technique. From the interfacial fluctuations, we have calculated the anisotropic interfacial stiffnesses with different critical parameter $\bar{\phi}_s$ and extracted the equilibrium interfacial stiffnesses of those crystal−melt interfaces. Fitting the interfacial stiffnesses to the equations given in Table 1, we calculated the average interfacial free energy $\gamma_0 = 0.62 \pm 0.02 k_BT/\sigma^2$ and the anisotropic parameters $\epsilon_1 = 0.056$ and $\epsilon_2 = -0.0073$. We find that the anisotropy of the interfacial free energy is weak and the interfacial free energies of different crystal−melt interface orientations are $\gamma_{100} = 0.64 \pm 0.02$, $\gamma_{110} = 0.62 \pm 0.02$, and $\gamma_{111} = 0.61 \pm 0.02 k_BT/\sigma^2$. Our results are in good agreement with the results of Davidchack and Larid,[29] based on the calculations of the reversible work required to create the interfaces. The anisotropic order is $\gamma_{100} > \gamma_{110} > \gamma_{111}$, which is similar to the results of the Lennard−Jones system.

However, we should point out that the results in current work are based upon a particular way to define the interface with a moderate system size and can be refined by more extensive calculations based on larger simulation systems in future work. Combined with the good agreement of a Lennard−Jones system between two different methods to determine the crystal−melt interfacial free energies,[17,26] it is reasonable to state that the capillary wave approach can be a reliable and efficient technique to calculate crystal−melt interfacial free energies.

References and Notes

(1) Pimpinelli, A.; Villain, J. *Physics of Crystal Growth*; Cambridge University Press: Cambridge, 1998.
(2) Hoyt, J. J.; Asta, M.; Karma, A. *Mater. Sci. Eng.* **2003**, *R41*, 121.
(3) Curtin, W. A. *Phys. Rev. Lett.* **1987**, *59*, 1228.
(4) Curtin, W. A. *Phys. Rev. B: Condens. Matter* **1989**, *39*, 6775.
(5) Marr, D. W.; Gast, A. P. *Phys. Rev. E: Stat. Phys., Plasmas, Fluids, Relat. Interdiscip. Top.* **1993**, *47*, 1212.
(6) Ohnesorge, R.; Lowen, H.; Wagner, H. *Phys. Rev. E: Stat. Phys., Plasmas, Fluids, Relat. Interdiscip. Top.* **1995**, *50*, 4801.
(7) Marr, D. W. *J. Chem. Phys.* **1995**, *102*, 8283.
(8) Turnbull, D. *J. Appl. Phys.* **1950**, *21*, 1022.
(9) Laird, B. B. *J. Chem. Phys.* **2001**, *115*, 2887.
(10) Smits, C.; van Duijneveldt, J. S.; Dhont, J. K. G.; Lekkerkerker, H. N. W.; Briels, W. J. *Phase Transitions* **1990**, *21*, 157.
(11) Underwood, S. M.; Taylor, J. R.; van Megen, W. *Langmuir* **1994**, *10*, 3550.
(12) Marr, D. W.; Gast, A. P. *Langmuir* **1994**, *10*, 1348.
(13) Glicksman, M. E.; Vold, C. *Acta Metall.* **1969**, *17*, 1.
(14) Napolitano, R. E.; Liu, S.; Trivedi, R. *Interface Sci.* **2002**, *10*, 217.
(15) Broughton, J. Q.; Gilmer, G. H. *J. Chem. Phys.* **1986**, *84*, 5759.
(16) Davidchack, R. L.; Laird, B. B. *Phys. Rev. Lett.* **2000**, *85*, 4751 and references therein.
(17) Davidchack, R. L.; Laird, B. B. *J. Chem. Phys.* **2003**, *118*, 7651.
(18) Lacasse, M. D.; Grest, G. S.; Levine, A. J. *Phys. Rev. Lett.* **1998**, *80*, 309.
(19) Sides, S. W.; Grest, G. S.; Lacasse, M. D. *Phys. Rev. E: Stat. Phys., Plasmas, Fluids, Relat. Interdiscip. Top.* **1999**, *60*, 6708.
(20) Chacón, E.; Tarazona, P. *Phys. Rev. Lett.* **2003**, *91*, 166103.
(21) Hoyt, J. J.; Asta, M.; Karma, A. *Phys. Rev. Lett.* **2001**, *86*, 5530.
(22) Morris, J. R.; Lu, Z. Y.; Ye, Y. Y.; Ho, K. M. *Interface Sci.* **2002**, *10*, 143.
(23) Hoyt, J. J.; Asta, M. *Phys. Rev. B: Condens. Matter* **2002**, *65*, 214106.
(24) Asta, M.; Hoyt, J. J.; Karma, A. *Phys. Rev. B: Condens. Matter* **2002**, *66*, 100101(R).
(25) Morris, J. R. *Phys. Rev. B: Condens. Matter* **2002**, *66*, 144104.
(26) Morris, J. R.; Song, Xueyu *J. Chem. Phys.* **2003**, *119*, 3920.
(27) Frenkel, D.; Smit, B. *Understanding Molecular Simulation: from algorithms to applications*; Academic Press: San Diego, CA, 1996.
(28) Cacciuto, A.; Auer, S.; Frenkel, D. *J. Chem. Phys.* **2003**, *119*, 7467.
(29) Laird, B. B. Private communication, revised simulations based on the cleaving method give the same order $\gamma_{100}(0.592) > \gamma_{110}(0.571) > \gamma_{111}(0.558)$ with somewhat lower numbers.